



# Yield prediction in banana (*Musa sp.*) using STELLA model

Adelaide Cristielle Barbosa da Silva<sup>1\*</sup>, Flávio Gonçalves Oliveira<sup>2</sup> and Ricardo Nuno da Fonseca Garcia Pereira Braga<sup>3</sup>

<sup>1</sup>Universidade Federal de Viçosa, Av. Peter Henry Rolfs, s/n, Campus Universitário, 36570-900, Viçosa, Minas Gerais, Brazil. <sup>2</sup>Instituto de Ciências Agrárias, Universidade Federal de Minas Gerais, Campus Regional de Montes Claros, Montes Claros, Minas Gerais, Brazil. <sup>3</sup>Instituto Superior de Agronomia, Universidade de Lisboa, Tapada da Ajuda, Lisboa, Portugal. \*Author for correspondence. E-mail: adelaide.silva@ufv.br

**ABSTRACT.** To overcome the challenges encountered in banana cultivation, such as the high cost of production due to high water consumption by the banana plant, efficient management practices are being adopted. The use of agricultural forecasting techniques is an alternative that has been gaining attention in rural areas. One way to manage and improve agricultural productivity is the use of technologies that allow the monitoring of production. The implementation of computational tools as software to aid processes, such as irrigation management, is gradually taking up space in the agricultural sector. In this light, herein, the present study aimed to develop a model using STELLA 8.0 software to estimate the growth and productivity of irrigated banana (*Musa sp.*). For this, the physiological processes and water demand were calculated using reference evapotranspiration ( $ET_0$ ) and culture evapotranspiration ( $ET_c$ ) in the first banana cycle for the climatic conditions of the Jaíba Project (Jaíba, Minas Gerais State, Brazil). The data of the climatic conditions were obtained from the National Institute of Meteorology. It was verified that the average monthly  $ET_0$  was  $5.78 \text{ mm day}^{-1}$ . In addition, the water requirement of the plant corresponded to a blade equivalent to 65% of  $ET_0$ . The verified productivity was  $8.93 \text{ t ha}^{-1}$ , which is considered adequate for the simulated conditions. The model responded efficiently to the proposed application and was characterized as a prognostic tool of reality through simplified representation.

**Keywords:** software; irrigation management; plant growth simulation.

Received on April 28, 2021.

Accepted on September 3, 2021.

## Introduction

Banana is prominent in world agriculture and is among the ten most produced and exported crops (FAO, 2015). It is one of the fruits present in the meals of the Brazilian population, demonstrating its relevance in the national agribusiness (Gonçalves et al., 2008).

With world productivity at around 117.9 million tons in 2015 (Kissel, van Asten, Swennen, Lorenzen, & Carpentier, 2015), the cultivation of bananas exhibited an expressive growth when compared to the world production in 2007 of only 70 million tons, according to Rodrigues and Leite (2008). However, according to Olivares et al. (2020), banana productivity varies depending on the producer country and variety of bananas.

According to Kissel et al. (2015), water scarcity is expected to affect the agricultural sector, thus causing evident droughts in areas planted with bananas. In most Brazilian regions where the fruit is produced, precipitation is insufficient, resulting in reduced fruit quality and quantity. Because the water consumption of the banana plant is high, it is essential to use irrigation to keep its tissues hydrated and meet its morphological needs.

Irrigated agriculture is one of the largest consumers of water on the planet (Christofidis, 2013). High agricultural water consumption is often associated with the low efficiency of water use systems, as well as the inapplicability of irrigation management methods (Bernardo, Mantovani, Silva, & Soares, 2019).

According to Coelho, Filho, and Oliveira (2005), the environmental sustainability of irrigated agriculture will only be possible if there is an efficient use of water to make irrigated projects feasible. This entails the management and adoption of appropriate management techniques, in addition to the implementation of new methodologies that favor their correct use.

According to Albuquerque (2012), the agricultural sector has a variety of computational tools for different functionalities and processes, including irrigated activity. Moreover, Jame and Cutforth (1996) considered the

technological progress of computing responsible for creating interactions by combining factors; in particular, quantitative organization of the soil, plants, and climatic conditions to accurately establish cultural productivity through simulation models.

The models are defined as a base formed by mathematical equations that reproduce a physical system, for example, the soil–water–atmosphere. It is possible to represent the performance of a culture in the field and estimate the growth of its constituents to quantitatively inform the fundamental processes for its growth and development. Thus, the validated model can be used as an instrument for agricultural forecasts and productivity management (Jame & Cutforth, 1996).

The crop yield models available on the market may present some limitations in the simulation of the data, owing to factors, such as the inadequacy of the type of culture to be modeled, lack of data validation and calibration, and the complexity of use.

The simplicity and practicality of STELLA characterize it as an efficient software for modeling and understanding complex systems. Researchers, such as Ouyang et al. (2014) and Ouyang (2008) have proven the effectiveness of the software in system dynamics.

The objective was to develop a simulation model capable of predicting the development, productivity, and water demand of the irrigated banana plant using a computational model developed by STELLA 8.0 software.

## Material and methods

STELLA 8.0 software (Isee Systems, 2017) was used to model the growth and production of the irrigated banana tree (*Musa* sp.). The field data for comparison between the simulation and experimental values were obtained from the studies by Figueiredo et al. (2006).

### Data Collection

The input data of the model referring to the environmental conditions were obtained from online databases, made available by the National Institute of Meteorology (INMET, 2017) of the Mocambinho Station, Minas Gerais State, Brazil. These data refer to the daily precipitation records, solar radiation, maximum and minimum temperatures, relative humidity, and wind speed, corresponding to the period from April 1999 to May 2001. The soil data were based on the characteristics of the sandy soil found in an area located in the Jaíba Project (15°20' S and 43°40' W), as described by Figueiredo (2006).

To determine the cultural coefficients of the different phenological phases, the values established by Figueiredo et al. (2006) were parameterized in comparison with the data recommended by Allen et al. (1998). The phases were defined based on the accumulated temperature (thermal integral), taking the base temperature and maximum temperature described by Coelho (2012) as the reference.

The water depth applied in the irrigation was obtained from the soil water balance, which refers to the difference between the inputs and outputs. Therefore, to determine the soil water balance, the values of crop evapotranspiration and precipitation data were considered.

### Model Structure

The architecture of the model consists of submodels, such as the soil water balance, thermal integral, liquid photosynthesis, dry plant weight, and organizational structure throughout the system.

The soil water balance submodel includes soil, climate, and crop conditions, as well as reference evapotranspiration (Penman–Monteith FAO 56 equation; Allen et al., 1998). The integral thermal submodel was based on modeling the phenological state of the banana from the accumulated temperature.

Productivity analysis was performed using the net photosynthesis and dry matter production submodel of the plant, involving cultural growth, calculation of gross and net photosynthesis, respiration, and partitioning of cultural components. All this information was defined for the temporal characterization in days.

### Soil Water Balance Submodel

To characterize this submodel, information regarding the field capacity, permanent wilt point, saturation point, and root depth of the banana tree was introduced. Soil water inflow was defined by infiltration, and the soil water outflow data were characterized by percolation, surface runoff, reference evapotranspiration ( $ET_0$ ), and culture evapotranspiration ( $ET_c$ ).  $ET_0$  was calculated from the following evapotranspiration equation (Penman–Monteith FAO 56 equation; Allen et al., 1998).

$$ET_0 = \frac{0,408 (Rn-G) + \gamma \frac{900}{T+273} u_2 (e_s - e_a)}{\Delta + \gamma(1 + 0,34 u_2)} \quad (1)$$

where:

- ET<sub>0</sub> - reference evapotranspiration (mm day<sup>-1</sup>);
- Rn - balance of radiation to the crop surface (MJ m<sup>-2</sup> day<sup>-1</sup>);
- G - soil heat flux density (MJ m<sup>-2</sup> day<sup>-1</sup>);
- T - air temperature at 2 m high (°C);
- u<sub>2</sub> - wind speed at 2 m in height (m s<sup>-1</sup>);
- e<sub>s</sub> - saturation vapor pressure (kPa);
- e<sub>a</sub> - partial vapor pressure (kPa);
- Δ - slope of saturation vapor pressure curve (kPa °C<sup>-1</sup>); and
- γ - psychrometric coefficient (kPa °C<sup>-1</sup>).

The culture evapotranspiration of the crop (ET<sub>c</sub>) was established from the reference evapotranspiration product (ET<sub>0</sub>) using the respective crop coefficient (K<sub>c</sub>) of the current phase of the plant. The adopted K<sub>c</sub> is characterized as a model parameter. In the case of water deficit, the coefficient of soil moisture deficit was considered in the calculation of ET<sub>0</sub>. The K<sub>c</sub> was divided into three phenological phases: K<sub>c1</sub>, K<sub>c3</sub>, and K<sub>c2</sub>. K<sub>c1</sub> and K<sub>c3</sub> are fixed values obtained from the calibration of the values indicated by Allen et al. (1998) and Figueredo et al. (2006), whereas K<sub>c2</sub> corresponds to a rising line representing phase II and is expressed as:

$$Kc_2 = Kc_1 + (Kc_3 - Kc_1) \times \frac{t}{X_2} \quad (2)$$

where:

- K<sub>c2</sub> - cultural coefficient of phase II;
- K<sub>c1</sub> - cultural coefficient of phase I;
- K<sub>c3</sub> - cultural coefficient of phase III;
- t - time from the start of phase II (d); and
- X<sub>2</sub> - duration of phase II (d).

The water content in the soil was determined by the balance between inflows and outflows. The inflows were characterized by precipitation and irrigation, while the outflows were characterized by drainage and evapotranspiration of the crop. Only the portion of the water from the precipitation that contributed to the reduction of the water deficit up to the limit of the field capacity was considered. Particularly, the water infiltration dynamic is effective when the soil water content is lower than the saturation moisture, a condition assumed for the inflow of water. For the outflow, the criterion adopted for the water lost through drainage refers to a water content greater than the moisture content of the field capacity.

Irrigation was carried out according to the needs observed with the results of this balance for theoretical purposes, as described by Figueiredo et al. (2006).

### Thermal integral submodel

The thermal integral or thermal accumulation used in the model was based on Equation (3), as established by Arnold (1959).

$$GD = \frac{(T_{max} + T_{min})}{2} \cdot T_b \quad (3)$$

where:

- GD - degrees-day (°C day<sup>-1</sup>);
- T<sub>max</sub> - maximum temperature (°C);
- T<sub>min</sub> - minimum temperature (°C); and
- T<sub>b</sub> - base temperature (°C).

To dynamize the model, the phenological state of the banana plant was defined by the difference between the thermal integral of each phase depending on the conditions of the place where the plant was inserted. Thus, to calculate the thermal integral, the values of base temperature (T<sub>b</sub>), average temperature (T<sub>med</sub>), and average duration (in days) were established. Accordingly, an approximate thermal duration (°C day<sup>-1</sup>) was obtained for each phase, as shown in Figure 1.

According to Robinson and Saúco (2010) and Coelho (2012), the base temperature for bananas is 14°C; however, Turner and Fortescue (2010) and Coelho (2012) classified vegetative zero at 13°C in the tropics.

Therefore, the value for the variable  $T_b$  was defined by the mean values proposed by the authors ( $13.5^\circ\text{C}$ ). The mean maximum temperature was approximately  $37^\circ\text{C}$  (Coelho, 2012) which was inserted into the base model.

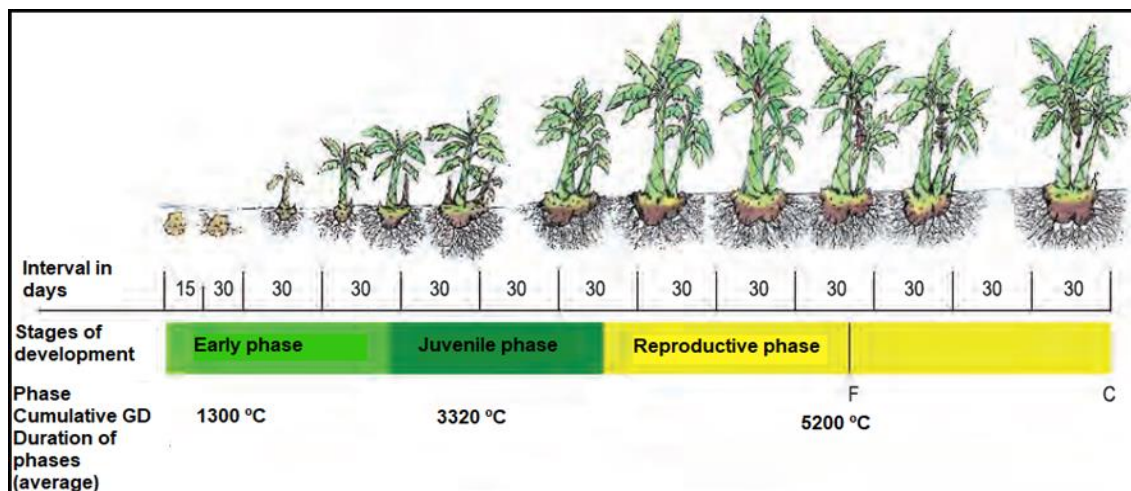


**Figure 1.** Schematic representation of the banana plant cycle. Durations of phenological phases for banana type Prata-anã. F = Emission of inflorescence; C = Harvest of the bunch; GD = Degree-day. Source: adapted from Coelho (2012).

### Net photosynthesis submodel

This submodel was developed by calculating the daily net photosynthesis, obtained from the difference between crude photosynthesis and respiration (Lakso & Johnson, 1990). Thus, Equation (4), which expresses the crude photosynthesis, was adapted from the exposition by Charles-Edwards (1982) as follows:

$$GP = RUE \times RAD \times [(1 - \exp(-k \cdot IAF))] \times FT \times FH_2O \quad (4)$$

where:

- GP - gross photosynthesis ( $\text{g CO}_2 \text{ m}^{-2} \text{ day}^{-1}$ );
- RUE - radiation use efficiency ( $\text{g MJ}^{-1}$ );
- RAD - incident solar radiation ( $\text{MJ m}^{-2}$ );
- k - canopy light extinction coefficient;
- IAF - leaf area index;
- FT - temperature factor; and
- $FH_2O$  - water availability factor.

The radiation use efficiency or the active photosynthetic efficiency used for the modeling was  $2.68 \text{ g MJ}^{-1}$  (Melo, Fernandes, Sobral, Brito, & Dantas, 2010). For the canopy light extinction coefficient, the value of 0.9 was accepted, because Coelho (2012) stated that "90% of the radiation is intercepted by the leaf canopy". The leaf area index was determined using Equation (5).

$$IAF = 2,357 \ln(\text{time}) - 10,30 \quad (5)$$

where time is calculated in days.

The temperature factor (FT) varied between 0 and 1. FT values were estimated from the FT versus  $T_{\text{méd}}$  plot, which represents the behavior of the plant in response to temperature in the following intervals:  $2\text{-}20^\circ\text{C}$  (linear increase of FT),  $20\text{-}25^\circ\text{C}$  ( $FT = 1$ ), and  $25\text{-}45^\circ\text{C}$  (linear decrease in FT).

The availability of water in the soil affects the photosynthetic process and is fully interconnected with plant development. When the soil moisture is in the field capacity, the value of  $FH_2O$  will be equal to 1. When there is a water deficit, the value of  $FH_2O$  will be equal to the coefficient of water stress ( $K_s$ ).

The determination of  $K_s$ , for converting  $E_{Tc}$  into actual crop evapotranspiration ( $E_{Tr}$ ), was based on the relationship proposed by Pierce, who concluded that  $E_{Tr}$  will remain above 90% of  $E_{Tc}$  as long as soil moisture is more than one-third of the available water; then, it will fall rapidly in an exponential form until the soil moisture reaches a permanent wilting point (Bernardo, Mantovani, Silva, & Soares, 2019).

Net photosynthesis was calculated as shown in Equation (6).

$$P_n = GP - GR \quad (6)$$

where:

P<sub>n</sub>- net photosynthesis (g CO<sub>2</sub> m<sup>-2</sup> day<sup>-1</sup>);

GP - gross photosynthesis (g CO<sub>2</sub> m<sup>-2</sup> day<sup>-1</sup>); and

GR - growth respiration (g CO<sub>2</sub> m<sup>-2</sup> day<sup>-1</sup>).

The respiration of growth was obtained from Equation (7) as follows:

$$GR = GP \times r_c \quad (7)$$

where  $r_c$  is the respiration coefficient.

The established value for the respiration coefficient was 0.05. This parameter was first estimated based on values taken from the literature, then calibrated for our data through numerical optimization (calibration).

### Dry matter production and distribution submodel

In this submodel, the weights of the dry plant biomass were determined. For each organ, a partition coefficient was defined for each phenological phase of the plant. The product of the partition coefficient and net photosynthesis corresponded to the growth of each organ.

The plant's dry matter is directly related to its growth and development within the cycle, assuming different values depending on the plant component. The partitioning of biomass or dry weight characterizes the growth differentiation process, as it is determined by coefficients that vary according to the phenological period. Thus, the partition coefficients were adjusted based on the plant's dry mass values described in the literature and subsequently calibrated for the model.

The inputs of this submodel were the initial weight and growth of the organ, and the outputs were the maintenance breath that was obtained by multiplying the organ weight, respiration coefficient, and temperature factor.

Based on the premise that each part has a different response to the weight and growth in each phase of the cycle, the partition coefficients assumed different values in each phenological phase, that is, 0.28 for the juvenile phase, 0.17 for the flowering phase, and 0.16 for the harvesting phase. For the stem, dry matter partition coefficients of 0.30, 0.40, and 0.39 were established, following the respective phases previously mentioned. The coefficients adopted for the root partition were 0.04, 0.04, and 0.02 for the juvenile, flowering, and harvesting phases, respectively. In the partition of the fruit, the value 0.25 was adopted, referring only to the stage of flowering when the fruits start filling.

### Statistics for model evaluation

According to Soltani and Sinclair (2012), some statistics can be used to test the robustness of a model, such as bias. Bias is obtained by calculating the average deviation between the model predictions and the system measurements as follows:

$$\text{Bias} = \sum(Y_i - X_i)/n$$

where  $X_i$  is the measured value,  $Y_i$  is the simulated value, and  $n$  is the number of pairs of measured and simulated values that are used in calculating bias.

The mean relative error (MRE) determines the magnitude of errors in relative terms and is expressed as a percentage of:

$$\text{MRE} = \frac{100}{n} \sum_{i=1}^n \left| \frac{O_i - P_i}{O_i} \right|$$

where  $O_i$  and  $P_i$  are the observed and predicted values by the model, respectively;  $n$  is the number of observations, and  $i$  is the time interval.

## Results and discussion

### Determination of Cultural Evapotranspiration (ET<sub>c</sub>)

The water requirement of the crop was obtained by calculating the evapotranspiration based on the climatic data of the Jaíba Project region for the simulated period. The cultural evapotranspiration was

calculated by multiplying the average monthly evapotranspiration value ( $ET_0$ ) by the  $K_c$  of the phenological phase of the plant. Thus, different values of cultural coefficients were attributed to the distributed months depicted in the Table 1 below, with the month of planting being December 1999.

**Table 1.** Distribution of  $K_c$ ,  $ET_0$  and  $ET_c$  in the banana plant cycle.

Plant age (month)	$K_c$	$ET_0$ (mm day <sup>-1</sup> )	$ET_c$ (mm day <sup>-1</sup> )
1	0.70	3.96	2.77
2	0.70	4.16	2.91
3	0.70	6.14	4.29
4	0.74	5.03	3.72
5	0.81	5.89	4.77
6	0.88	5.52	4.86
7	0.95	5.39	5.12
8	1.02	5.87	5.98
9	1.09	7.53	8.20
10	1.10	7.66	8.42
11	1.10	7.95	8.74
12	1.10	4.44	4.88
13	1.10	3.24	3.56
14	1.10	6.94	7.63
15	1.10	6.95	7.64

The results of the crop coefficients were higher than those recommended by the FAO, ranging from 0.56 to 0.85. However, the values were close to those recommended by Allen et al. (1998), which established a variation between 0.5 and 1.1. There was only a subtle difference in the initial  $K_c$ , which was higher than the recommended value. However, it resembles the initial  $K_c$  obtained by Figueiredo et al. (2006) of 0.71, while the region analyzed by the author corresponds to the one simulated in the model with the climatic data referring to the same evaluation period.

The higher the frequency of irrigation, the higher the initial  $K_c$  (Bernardo, Soares, & Mantovani, 2008), considering that frequency of irrigation depends on the evapotranspiration demanded and the soil moisture of the site. Based on the values defined for  $K_c$ , the respective  $ET_c$  values were obtained, as shown next to the reference evapotranspiration ( $ET_0$ ) in Figure 2.

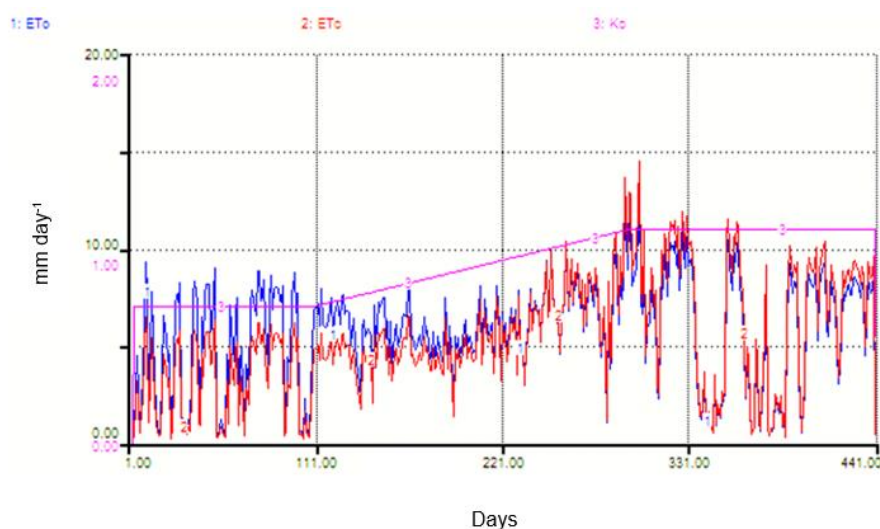


**Figure 2.** Reference evapotranspiration ( $ET_0$ ) and culture evapotranspiration of the crop ( $ET_c$ ) throughout the cycle. In the graph, the blue line (1) depicts reference evapotranspiration, the red line (2) characterizes the crop evapotranspiration, and the pink line (3) represents the distribution of the cultural coefficients.

The average reference evapotranspiration ( $ET_0$ ) simulated by the model during the first cycle of the plant was 5.78 mm day<sup>-1</sup>. This value is close to the usual value (5.5 mm day<sup>-1</sup>) obtained in the region according to Figueiredo (2006). This small variation may be due to the climatic variability that occurs every year and the difference in climatic seasons in which the data were collected.

In the hottest months of the year in the region (August, September, and October), the highest evapotranspiration values were observed. The evapotranspiration of the crop was highest in October, which is the eleventh month of the plant age, as shown in Table 1. This response is due to the climatic conditions of the region because October is characterized as the driest month.

Bezerra et al. (2017) proved the high evapotranspiration value of crops in the driest month. The authors pointed out that the region of Missão Velha, located in the state of Ceará (Brazil), which has the same climatic characteristics as the simulated region, showed the highest evapotranspiration rate of the banana in October and November.

The water demand was characterized by the accumulation of crop evapotranspiration ( $ET_c$ ) during the simulated period, which corresponded to 2,360 mm. This result is within the expected range for the banana tree because the crop requires consumption of approximately 150 to 200 mm of water per month as stated by Coelho (2012). Furthermore, the water consumption is dependent on different conditions (climate, soil, irrigation management) to which the plant is submitted.

In addition, Figueiredo (2006) obtained a similar water requirement, corresponding to 1,999.43 mm. The quantity of irrigated water in the simulation, intended to meet the water requirements of the crop, was equivalent to approximately 65% of  $ET_0$ .

### Soil characteristics and water content

The soil water balance submodel is represented by a flowchart, also called the Forrester diagram (Forrester, 1992). It describes the schematization of the model by levels and flows, as presented in Figure 3.

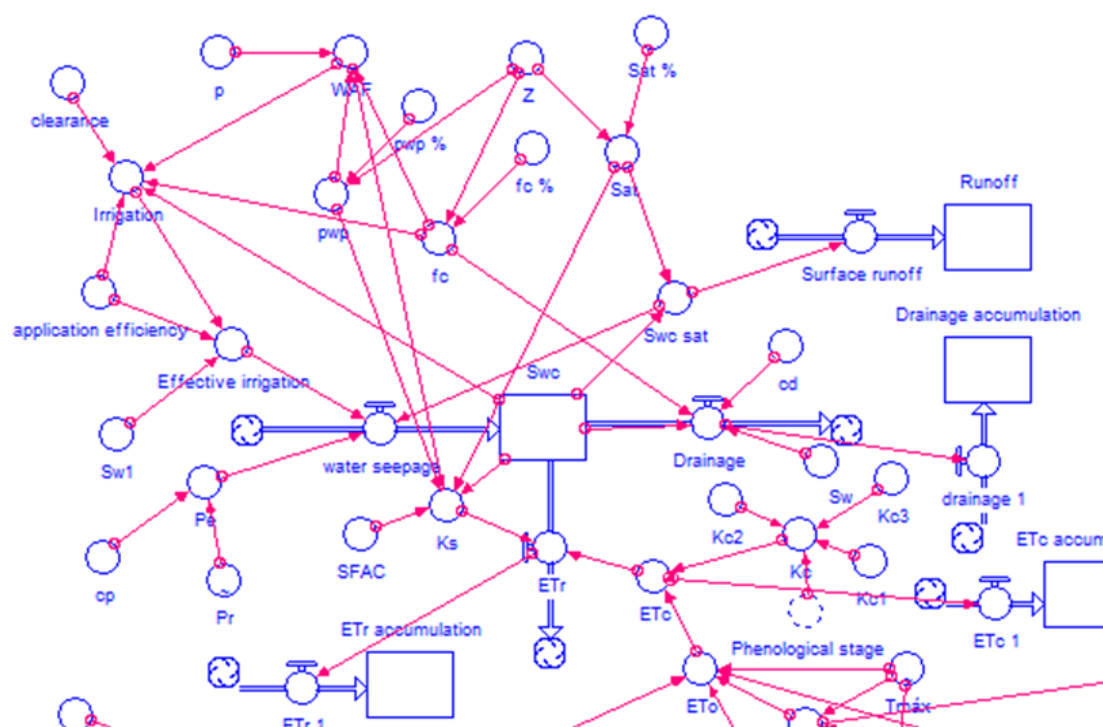


**Figure 3.** Structure of the soil water balance in the soil by STELLA 8.0 software. Scheme for describing soil water balance, where Swc corresponds to soil water content, fc - field capacity (mm), pwp - permanent wilting point (mm), p - availability factor, Z - root depth (mm), WAF - water availability factor, and Sat is the saturation of soil water.

The simulated soil is characterized as sandy, with the values of field capacity and permanent wilting point corresponding to 8.72% and 2.37% of humidity, respectively. The effective depth of the root system was assumed to be 30 cm. These values were based on a study by Figueiredo (2006). Thus, the water availability factor (WAF) of soil water (mm) was determined. As shown in Figure 4, the value of the blade to be irrigated was calculated to prevent water deficit and maintain the plants in water availability factor (WAF) of soil water (mm).

The soil water limit was 16.93 mm, which was satisfactory when compared to the 16.7 mm value found by Figueiredo (2006). The water layer applied to the soil was 17.60 mm, considering a gap related to the average  $ET_0$ . This value is slightly higher than that used by Figueiredo (2006), with a difference of 20%. This behavior may be associated with the difference in some readings of climatic conditions of the analyzed period because

the climatic data collected by the author came from an automatic station installed at the planting site. In addition, the mean  $ET_0$  observed by Figueiredo (2006) was lower than that reported previously. Thus, high consumption of water by evapotranspiration results in high demand for water to supply the needs of the plant. A few blue peaks are observed in the graph presented in Figure 4, referring to the elevation of soil water content (Swc), which is justified by the concentration of rain in this interval.

Figure 5 shows the amount of rain during the period simulated by the software. It was verified that there was a greater concentration of rain in the months of January, October, and December than in the other months. This indicates that there is a great need for irrigation to meet the water demand of crops in the region.

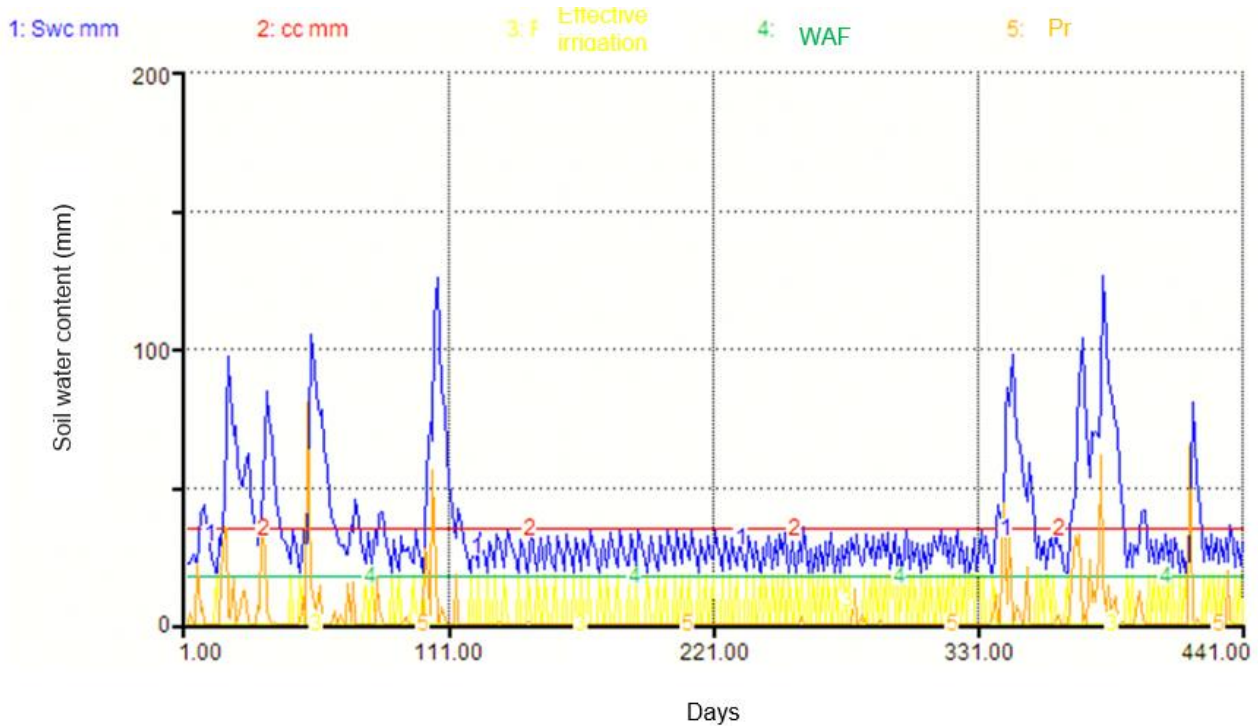


**Figure 4.** Soil water balance using STELLA 8.0 software. Graphical representation of the water limits in the soil where 1 - Swc - Water content in the soil (blue line) at a depth of 30 cm, 2 - fc - Field capacity (red line), 3 - Effective irrigation (yellow line); 4 - WAF - Water availability factor (green line), and 5 - Pr - Precipitation (orange line).

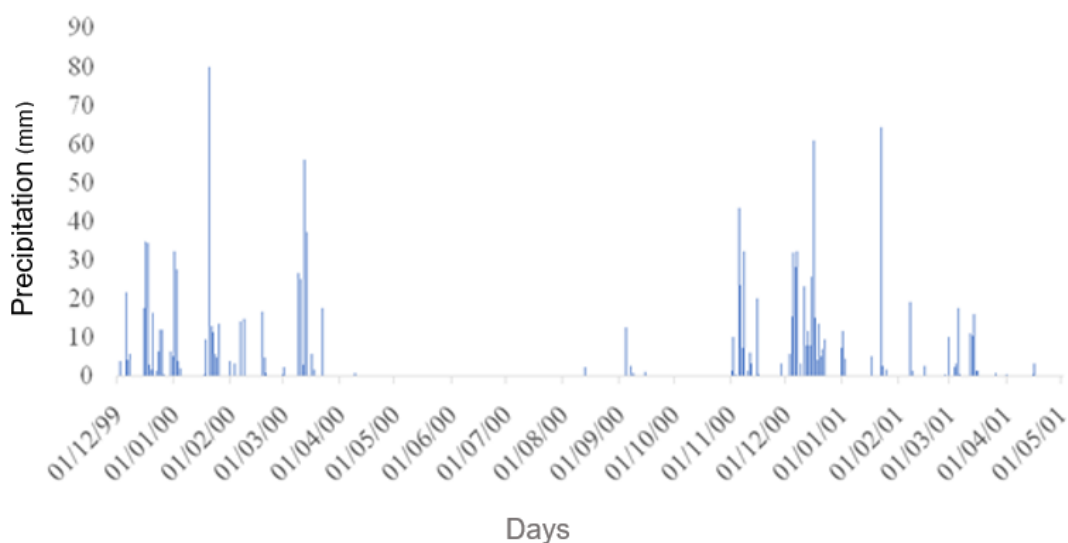


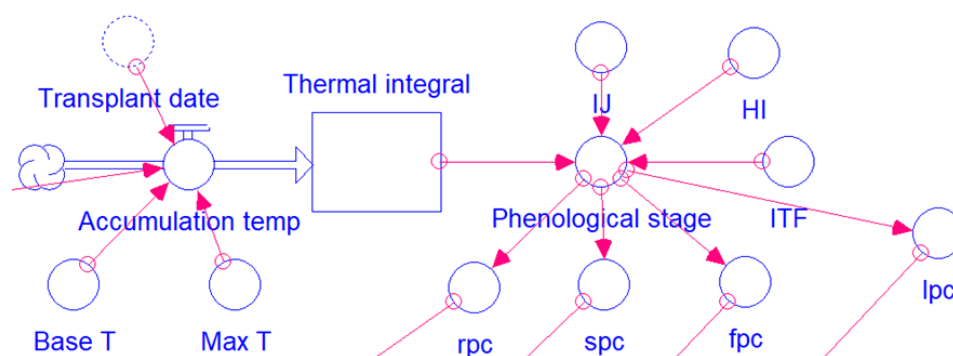
**Figure 5.** Precipitation values of the Jaiba Project from December 1999 to April 2001.

### Phenological indices from the thermal integral

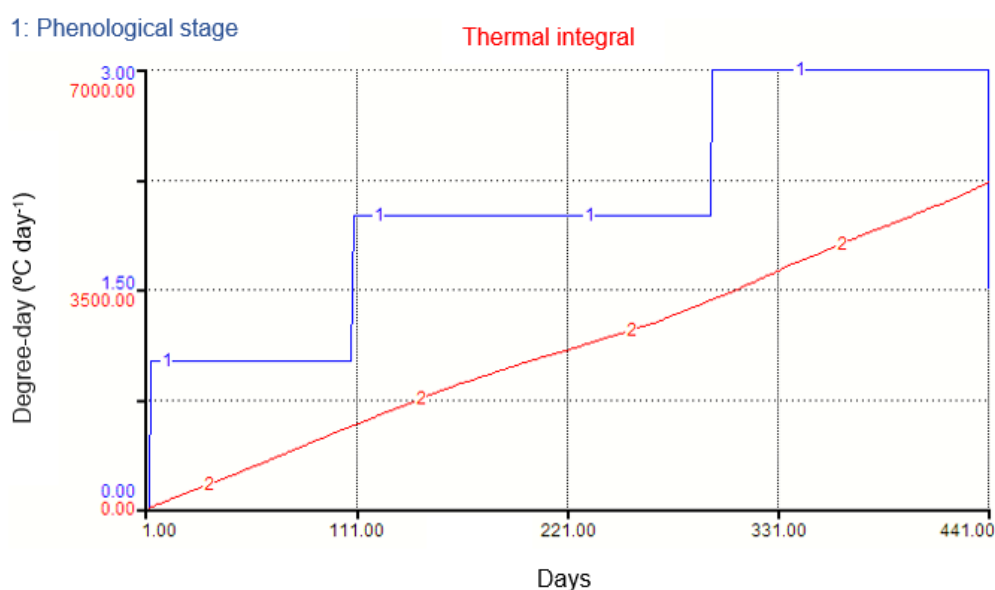
The phenological distribution corresponding to the amount of temperature accumulated at each stage of the plant was obtained, as illustrated in Figure 1.



Figure 6 illustrates the following variables that describe the classification of phenological stages: Base T - base Temperature (13.5°C); Med T - average temperature (according to climatic data of the simulated period) and Max T - maximum temperature (37°C). The increasing trend of the thermal integral in the cycle associated with the distribution of the phenological phases can be observed in Figure 7. The values defined according to the phenological division in degree-day ( $^{\circ}\text{C day}^{-1}$ ) for juvenile, flowering, and harvesting phases were 1,300 $^{\circ}\text{C day}^{-1}$ , 3,320 $^{\circ}\text{C day}^{-1}$ , and 5,200 $^{\circ}\text{C day}^{-1}$ , respectively.



**Figure 6.** Interface of the temperature accumulation process using STELLA 8.0 software. Structure of the dynamics of the division of the phenological stages of the first cycle of the banana plant. ITF - Integral of flowering, IJ - Integral juvenile, HI - Harvest Integral.



**Figure 7.** Distribution of the phenological stage of the plant based on the thermal integral. In the graphical representation, the blue line (1) refers to the phenological stage, with the three constant lines representing the juvenile, flowering, and harvesting phases, respectively. The red line (2) characterizes the increase in the thermal integral.

The degree-day values differed from the values established by Figueiredo (2006). The authors obtained shorter phases with smaller thermal integrals. However, according to Coelho (2012), the average temperature for the crop cycle is 27°C, which is close to the simulated mean temperature of 28°C.

### Photosynthesis and dry matter partition

The plant growth was provided based on the net photosynthesis and dry matter production submodels of the plant, in which the partition coefficients for the plant organs were determined. As shown in Figure 8, few divergences were observed between gross and net photosynthesis because net photosynthesis is only influenced by plant respiration.

From Figure 8, it can be observed that the photosynthetic rate is affected by the light incidence which increases proportionally. This idea was reinforced by Coelho (2012) who stated that CO<sub>2</sub> retained per square meter of soil occupied by the canopy increases with increasing light.

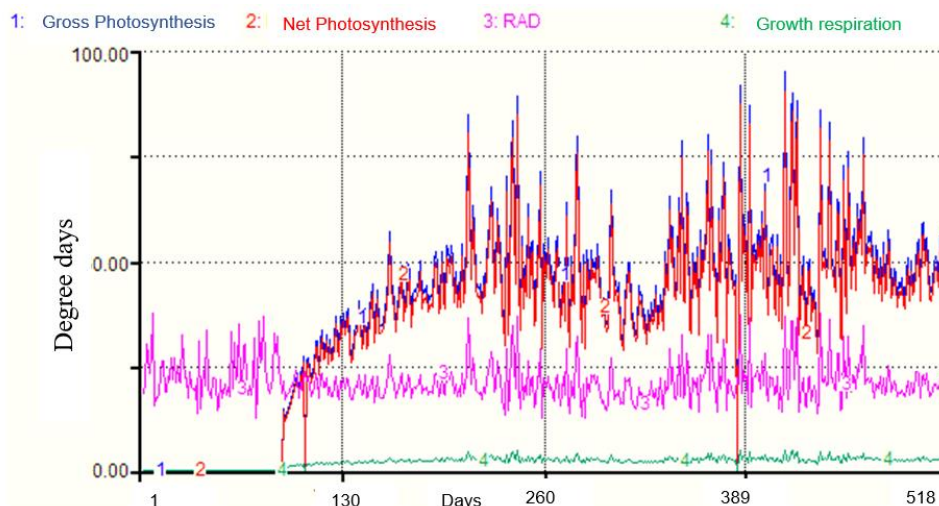


**Figure 8.** Effect of radiation on the behavior of net photosynthesis. The graphical representation illustrates the following: 1 - Gross photosynthesis (blue line), 2 - Net photosynthesis (red line), 3 - RAD - extraterrestrial solar radiation (pink line), and 4 - Rate of growth respiration (green line).

From the net photosynthesis, it was possible to determine the dry matter for the plant organs, as shown in Figure 9, using the Forrester diagram (Forrester, 1992). This was built on the dry matter production submodel of the plant, resulting in the values described in Table 2.

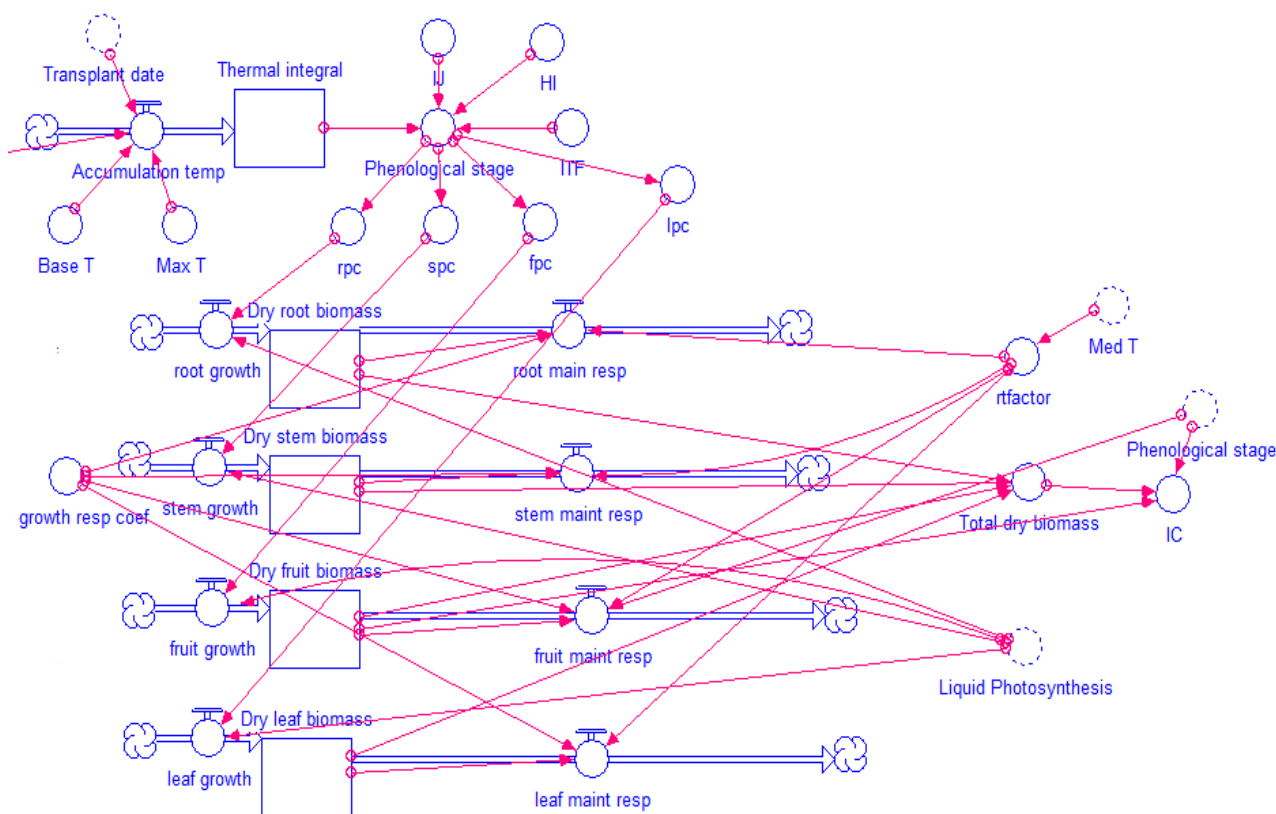


**Figure 9.** Dry matter for the plant organs using STELLA 8.0 software. Forrester diagram for the simulated dry matter partitioning of different organs.

**Table 2.** Distribution of the dry matter values of the aerial parts of the plant.

Value given by	Dry biomass (g plant <sup>-1</sup> )		
	Leaf	Stem	Fruit
Melo et al. (2010)	953.77	2,305.84	1,662.11
Simulated	964.00	2,315.00	1,689.00
MRE (%)	1.07	0.40	1.62

Interconnections with the other submodels is demonstrated by the graph generated in Figure 10, which characterizes the growth of each part of the plant throughout the first cycle.

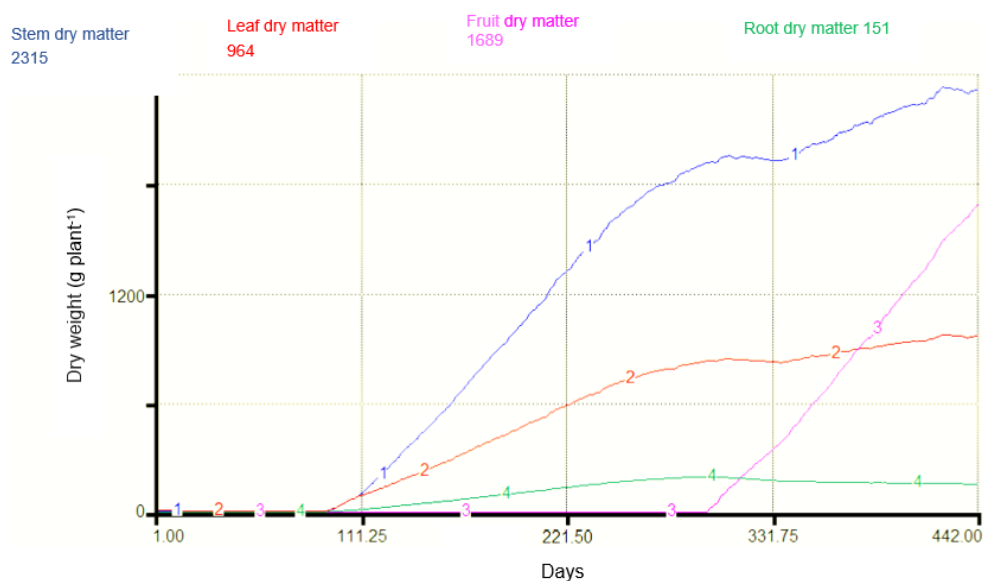


**Figure 10.** Dry matter of vegetative organs of the plant. The graph illustrates the dry matter production and distribution between plant tissues as follows: 1 - stem dry matter (blue line), 2 - leaf dry matter (red line), 3 - fruit dry matter (pink line), and 4 - root dry matter (green line).

The simulated dry matter values were compared with those observed in the field by Melo et al. (2010), who studied in detail the growth and development of the organs of the cultivar Prata-Anã, conducted under similar experimental conditions. However, Melo et al. (2010) considered the effects of nutrients on plant growth.

The dry matter response is satisfactory because it is similar to the values highlighted by Melo et al. (2010), as evidenced by the low MRE values shown in Table 2. Thus, from the dry matter production, a moist bunch with a weight of 6.70 kg was obtained because the moisture content of the banana was 74.8% (Bezerra & Dias, 2009).

An estimated productivity of 11,169 kg ha<sup>-1</sup> was obtained for the 3.0 x 2.0 m spacing (1,667 seedlings ha<sup>-1</sup>). According to Pereira et al. (2000), this is the most appropriate spacing for the first production cycle in the Jaíba region.

However, considering the 3.0 x 2.5 m spacing used by Figueiredo (2006), the productivity reached in the model was 8.93 t ha<sup>-1</sup> which is lower but close to the productive average of 9.32 t ha<sup>-1</sup> verified by the author, for the mean of the irrigated blade of water of 60-80% ET<sub>0</sub>. Accordingly, it is justified that the simulated productivity is adequate for the crop because the productivity in the first cycle is inferior (Coelho, 2012) with a bias of 0.39 from the model, which indicates a good fit of the data.

## Conclusion

The analysis of shoot dry biomass values (leaf phytomass + stem biomass + fruit phytomass) found in the simulation of STELLA 8.0 corroborates the efficiency of plant modeling growth and production. The simulation of the water demand of the culture matches the assumptions through the simplified representation of reality by obtaining satisfactory values when compared with the real ones. The results of the dry weights of the plant in relation to productivity achieved the objective proposed in the model, with acceptable values. However, the simulation of the thermal integral should be better adjusted for the cycle, considering that simulation of the thermal integral submodel was based on only a small range of climatic data and does not represent the history of years in the region. The crop productivity model is characterized as an efficient tool for agricultural optimization and management, emphasizing the possibility of predicting future events based on past data.

## References

Albuquerque, P. E. P. (2012). *O Aplicativo Computacional "Irrigafácil" Implementado Via Web para o Manejo de Irrigação dos Campos Experimentais da Embrapa Milho e Sorgo*. Sete Lagoas, MG: Embrapa Milho e Sorgo. Retrieved on April 30, 2017 from <https://bitlybr.com/yPtPg>

- Allen, R. G., Pereira, L. S., Raes, D., & Smith, M. (1998). *Crop evapotranspiration: Guidelines for computing crop water requirements*. Rome, IT: FAO. (Fao Irrigation Drainage paper, 56).
- Arnold, C. Y. (1959). The determination and significance of the base temperature in a linear heat unit system. *Proceedings of the American Society for Horticultural Science*, 74(1), 430-445.
- Bernardo, S.; Mantovani, E. C.; Silva, D. D. & Soares, A. A. (2019). *Manual de irrigação* (9. ed.). Viçosa, MG: UFV.
- Bernardo, S.; Soares, A. A. & Mantovani, E. C. (2008). *Manual de irrigação* (8. ed.). Viçosa, MG: UFV.
- Bezerra, A. E., Oliveira, C. W., Neto, J. M. M., Silva, T. I., Meireles, A. C. M., & Santos, H. R. (2017). Eficiência do uso da água de irrigação no cultivo de banana (*Musa sp. L.*). *Revista Brasileira de Agricultura Irrigada*. 11(7), 1966-974. DOI: <https://doi.org/0.7127/rbai.v11n700663>
- Bezerra, V. S., & Dias, J. S. A. (2009). Avaliação físico-química de frutos de bananeiras. *Acta Amazonica*, 39(2), 423-428.
- Charles-Edwards, D. A. (1982). *Physiological determinants of crop growth*. Sydney, AU: Academic Press.
- Christofidis, D. (2013). Água, irrigação e agropecuária sustentável. *Revista de Política Agrícola*, 22(1), 115-127.
- Coelho, E. F. (2012). *Irrigação da bananeira*. Brasília, DF: Embrapa.
- Coelho, E. F., Filho, M. A. C., & Oliveira, S. L. (2005). Agricultura irrigada: eficiência de irrigação e de uso de água. *Bahia Agrícola*, 7(1), 57-60.
- FAO (2015). *Climate change and food systems: global assessments and implications for food security and trade*. Rome, IT: Food Agriculture Organization of the United Nations (FAO).
- Figueiredo, F. P., Mantovani, E. C., Soares, A. A., Costa, I. C., Ramos, M. M., & Oliveira, F. G. (2006). Produtividade e qualidade da banana prata-anã, influenciada por lâminas de água, cultivada no Norte de Minas Gerais. *Revista Brasileira de Engenharia Agrícola e Ambiental*, 10(4), 798-803.
- Forrester, J. W. (1992). Policies, decisions and information-sources for modeling. *European Journal of Operational Research*, 59(1), 42-63. DOI: [https://doi.org/10.1016/0377-2217\(92\)90006-U](https://doi.org/10.1016/0377-2217(92)90006-U)
- Gonçalves, V. D., Nietsche, S., Pereira, M. C. T., Silva, S. O., Santos, T. M., Oliveira, J.R., ... Ruggiero, C. (2008). Avaliação das cultivares de bananeira Prata-Anã, ThapMaeo e Caipira em diferentes sistemas de plantio no Norte de Minas Gerais. *Revista Brasileira de Fruticultura*, 30(2), 371-376. DOI: <https://doi.org/10.1590/S0100-29452008000200018>
- Isee Systems. (2017). *Systems thinking in education*. Retrieved on May 15, 2017 from <https://www.iseesystems.com>
- Instituto Nacional de Meteorologia [INMET]. (2017). *Estações Automáticas*. Retrieved on Jan. 26, 2017 from <http://www.inmet.gov.br/portal/index.php?r=estacoes/estacoesautomaticas>
- Jame, Y. W., & Cutforth, H. W. (1996). Crop growth models for decision support systems. *Canadian Journal of Plant Science*, 76(1), 9-19.
- Kissel, E., van Asten, P., Swennen, R., Lorenzen, J., & Carpentier, S. C. (2015). Transpiration efficiency versus growth: Exploring the banana biodiversity for drought tolerance. *Scientia Horticulturae*, 185, 175-182. DOI: <https://doi.org/10.1016/j.scienta.2015.01.035>
- Lakso, A. N., & Johnson, R. S. (1990). A simplified dry matter production model for apple using automatic programming simulation software. *Acta Horticulturae*, 276, 141-148. DOI: <https://doi.org/10.17660/ActaHortic.1990.276.15>
- Melo, A. S., Fernandes, P. D., Sobral, L. F., Brito, M. E. B., & Dantas, J. D. M. (2010). Growth, biomass yield and photosynthetic efficiency of banana, under fertirrigation with nitrogen and potassium. *Revista Ciência Agronômica*, 1(3), 417-426. DOI: <https://doi.org/10.1590/S1806-66902010000300014>
- Olivares, B. O., Araya-Alman, M., Acevedo-Opazo, C., Rey, J. C., Cañete-Salinas, P., Kurina, F. G., ... & Gómez, J. A. (2020). Relationship between soil properties and banana productivity in the two main cultivation areas in Venezuela. *Journal of Soil Science and Plant Nutrition*, 20, 2512-2524.
- Ouyang, Y. (2008). Modeling the mechanisms for uptake and translocation of dioxane in a soil-plant ecosystem with STELLA. *Journal of Contaminant Hydrology*, 95(1-2), 17-29. DOI: <https://doi.org/10.1016/j.jconhyd.2007.07.010>
- Ouyang, Y., Zhang, J., Leininger, T. D., & Frey, B. R. (2014). A STELLA model to estimate water and nitrogen dynamics in a short-rotation woody crop plantation. *Journal of Environment Quality*, 44(1), 200-209. DOI: <https://doi.org/10.2134/jeq2014.01.0015>

- Pereira, M. C. T., Salomão, L. C. C., Silva, S. O., Sedyama, C. S., Couto, F. A. A., & Neto, S. P. S. (2000). Crescimento e produção de primeiro ciclo da bananeira 'Prata Anã'(AAB) em sete espaçamentos. *Pesquisa Agropecuária Brasileira*, 35(7), 1377-1387. DOI: <https://doi.org/10.1590/S0100-204X2000000700012>
- Robinson, J. C., & Saúco, V. G. (2010). *Bananas and plantains: Crop production science in horticulture* (2nd ed.). Oxford, UK: CAB International.
- Rodrigues, M. G. V., & Leite, M. A. V. (2008). Aspectos socioeconômicos da bananicultura. *Informe Agropecuário*, 29(245), 7-12.
- Soltani, A., & Sinclair, T. R. (2012). *Modeling physiology of crop development, growth and yield*. Wallingford, UK: CABI.
- Turner, D. W., & Fortescue, J. A. (2010). The physiology of banana (*Musa* spp.) fruit growth: factors that affect bunch initiation. In Reunión de la Asociación para la Cooperación em Investigación y Desarrollo Integral de las Musáceas, *Banano y plátano* (p. 291-296). Medellín, CO: ACORBAT.